Synthesis of Hyperbranched Poly(aryl ether)s via Carbene Insertion Processes

Anton Blencowe,† Nick Caiulo,† Kevin Cosstick,‡ William Fagour,† Peter Heath,† and Wayne Hayes*,†

The School of Chemistry, The University of Reading, Whiteknights, Reading RG6 6AD, UK, and DuPont-Invista (UK), P.O. Box 401, Wilton Site, Middlesbrough, Cleveland TS6 8JJ, UK

Received August 23, 2006; Revised Manuscript Received December 4, 2006

ABSTRACT: Homopolymerization of alkylarylcarbenes derived from diazirine monomers that featured benzyl alcohol or phenol residues was found to lead to the production of soluble hyperbranched poly(aryl ether)s. The polymerization process was influenced by the solvents employed, monomer concentration, and the reaction time. An increase in the monomer concentration and reaction time was found to lead to an increase in the molecular weight characteristics of the resulting polymers as determined by gel permeation chromatography (GPC). The composition and architecture of the polyethers were determined by nuclear magnetic resonance (NMR) spectroscopic analysis and were found to be highly complex and dependent on the structure of the monomers used. All of the polymers were found to contain ether linkages formed via carbene insertion into O−H bonds, although polymers derived from phenolic carbenes also contained linkages arising from C-alkylation.

Introduction

Carbenes are highly reactive electron-deficient carbon-containing species that have found widespread use in synthetic organic chemistries,[1] surface modification, and biological applications.[2] Recently, Moloney and co-workers have employed carbenes derived from aryldiazomethanes to attach anchors onto various substrates by which dyes were incorporated onto the substrate.[3] The diarylcarbenes generated in this process were utilized for the functionalization of substrates such as nylon, polystyrene, and even polytetrafluoroethylene, thus demonstrating the high reactivity of carbene-containing species. In comparison, Hayes and co-workers have reported a rather more direct approach for the modification of nylon using carbenes generated from a diazirine functionalized fluorenone.[4] In contrast, "free" carbenes have been utilized rarely to construct polymeric materials as a result of the poor selectivity and unpredictable nature of these reagents. The synthesis of polymers using carbene precursors such as diazoalkanes and aryldiazomethanes has been well documented, although in the majority of cases "free" carbenes are not involved in the process. The polymerization of diazomethane using boron catalysts such as tetraacetyl diborate,[5] alkyl borates,[6,7] boron halides,[8−11] trialkylboranes,[12,13] and diborane[14] to prepare high molecular weight polymethylidene was first reported by Meerwein.[5] Boron catalysts have also been employed to synthesize polybenzylidene from phenyldiazomethane[15] and random copolymers[16] and cross-linked networks[17] from diazomethane and other diazoalkanes. For example, the copolymerization of diazomethane and 9-anthryldiazomethane afforded a luminescent polymethylidene copolymer.[18] Recently, Shea and co-workers have utilized boron catalysis to produce poly(ethylacetalmethylidene) oligomers from ethyl diazoacetate.[19] Boron-catalyzed polymerizations of this nature[20] proceed via initial nucleophilic attack of the diazoalkane on the borane center to form a borate complex that undergoes a 1,2-migration accompanied by loss of nitrogen and formation of an alkylborane.[21−23] Repetition of this process affords a polymer without the formation of "free" carbenes. A variety of metals and metal salts[5,11,24,25] have also been exploited to synthesize polymers from diazoalkanes, including colloidal metallic gold, which was found to have stereospecific regulating properties leading to the formation of highly crystalline polyethylidene from diazoethane.[26] This type of polymerization involves carbenoid type species[27] and is comparable to the Fischer−Tropsch reaction[28,29] in which polymerization of methylene groups occurs on metal surfaces.

In comparison to polymerization of carbenoid-type diazoalkane systems, it has been proposed that thermal polymerization of aryldiazoalkanes proceeds via the formation of "free" carbenes to yield polybenzylidenes with degrees of polymerization of up to 71.[30] Initially, the aryldiazoalkanes were generated in situ by the treatment of sodium hydroxide on tosylhydrazones in heterogeneous solvent systems and then thermally decomposed to afford polymers with number-average molecular weights (M_n) between 0.7 and 11.0 kDa. In addition, the thermal decomposition of *p*-mercaptophenyldiazomethane derivatives was reported[30] to yield polythioethers (Scheme 1) with degrees of polymerization ranging from 18 to 24 via the insertion of carbenes into the sulfur−hydrogen bonds.

To date, the only report of a polymerization involving diazirines is the photoinduced homopolymerization of anhydrous diazirine (methylenediazirine) in the gas phase or in inert solvents to afford complex polymethylene structures.[31] As the only reactive intermediate present in the process was methylene carbene ($:CH_2$), then polymerization occurred through its reaction with other methylene carbenes, unphotolyzed diazirine, or via insertion into preformed products. Electrospray mass spectrometry of the polymers displayed a complicated pattern of peaks ranging up to 500 Da and containing a repeat pattern of 14 Da that is consistent with multiple insertion of methylene carbene into smaller molecules thus formed.

As part of a program investigating carbene insertion polymerization methodologies, we have studied the construction of polymeric materials using arylcarbenes derived from the photoinduced decomposition of diazirines. Herein, we report the synthesis of several hydroxyl functionalized diazirine monomers

* Corresponding author. E-mail: w.c.hayes@reading.ac.uk.
† The University of Reading.
‡ DuPont-Invista (UK).

10.1021/ma061951l CCC: $37.00
Published on Web 01/20/2007

Scheme 1. Thermal Polymerization of *p*-Mercaptophenyldiazomethane; (a) Δ, Dimethylformamide, or Pyridine[30]

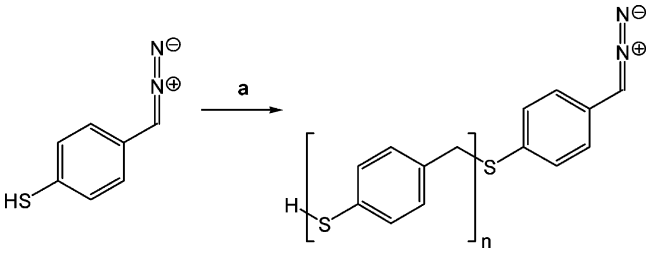

and their photoinduced polymerization under a variety of conditions to afford hyperbranched polyether architectures.

Results and Discussion

Monomer Synthesis. A small family of hydroxyl functionalized monomers (**1**−**4**, Figure 1) based on 3-aryldiazirines were constructed at the outset. Both 3-methyl- and 3-(trifluoromethyl)-diazirine monomers were developed in order to determine the effect, if any, that the carbene type has upon the polymerization process.

3-Methyldiazirine **1** was synthesized from 3-hydroxyacetophenone in five steps with an overall yield of 49%. At the outset, the hydroxyl group of 3-hydroxyacetophenone was protected as the tetrahydropyranyl (THP) ether **5**[32] (Scheme 2) through reaction with 3,4-dihydro-2*H*-pyran in the presence of pyridinium-*p*-toluenesulfonate (PPTS). The acetophenone derivative **5** was then converted via reaction with benzylamine into the corresponding *N*-benzylimine. Reaction of the *N*-benzylimine with hydroxylamine-*O*-sulfonic acid (HOSA) in liquid ammonia at −78 °C followed by oxidation with triethylamine and iodine afforded the protected 3-methyldiazirine **6** as an oil. Removal of the protecting group using *p*-toluenesulfonic acid (PTSA)[33] resulted in considerable decomposition of the diazirine function, and therefore, a milder proton source provided by hydroxylamine hydrochloride was exploited. The deprotected diazirine, 3-(3-hydroxyphenyl)-3-methyldiazirine **1**, was obtained as a white solid after column chromatography.

The 3-(trifluoromethyl)diazirines **2**−**4** were synthesized efficiently starting from the aryl bromide precursors **7**−**9** (Scheme 3), respectively. Aryl bromide **9** was synthesized from 3-bromophenol and methyl iodide in KOH saturated THF.[4] Substitution of the bromine in **7**−**9** with *N*,*N*-diethyltrifluoroacetamide via transmetallation with *n*-BuLi afforded the trifluoromethyl ketones **10**−**12**, respectively. Reaction of the ketones **10**−**12** with hydroxylamine hydrochloride resulted in formation of the oximes **13**−**15**, which were then tosylated to afford the corresponding tosyl oximes **16**−**18**, respectively. Amination and displacement of the tosyl groups by ammonia resulted in formation of the diaziridines **19**−**21** which were subsequently oxidized using silver(I) oxide to give the desired diazirines **22**−**24**, respectively.

Deprotection of the hydroxyl groups present in phenolic diazirines **22** and **23** using boron tribromide afforded the phenolic diazirines **2** (78% over seven steps) and **3** (81% over six steps), respectively. 3-(3-Methylphenyl)diazirine **24** was converted into the 3-(3-(hydroxymethyl)phenyl)diazirine derivative **4** via the benzyl bromide **25** (Scheme 4). Reaction of **24** with *N*-bromosuccinimide (NBS) in the presence of the radical initiator 1,1′-azobis(cyclohexane−carbonitrile) afforded the crude benzyl bromide **25**, which was hydrolyzed using silver nitrate in 1:1 water:dioxane to afford the diazirine **4** (47% over eight steps).

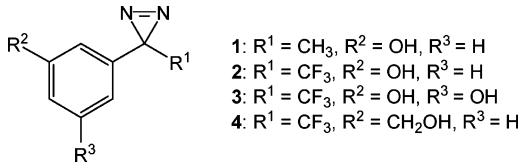

Figure 1. Structures of diazirine functionalized monomers **1**−**4**.

Scheme 2. Synthesis of the AB-Type 3-Methyldiazirine Monomer 1: (a) (i) NH_2Bn, $ZnCl_2$, (ii) NH_3, HOSA, (iii) I_2, NEt_3; (b) NH_2OH·HCl

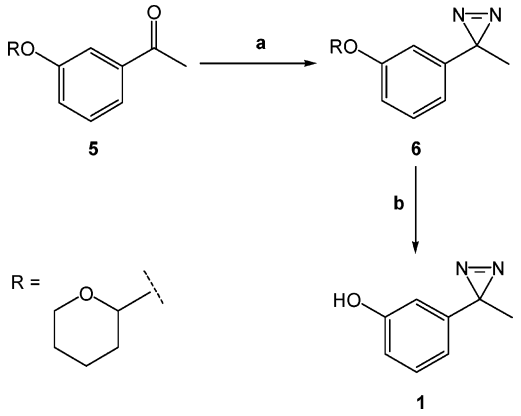

Polyether Synthesis and Characterization. The photochemical polymerization of the diazirine monomers **1**−**4** was conducted in the bulk and in the solution phase within a set concentration range (0.23−0.68 M) for a period of 24 h using a 125 W high-pressure mercury vapor lamp. After isolation the resulting polymers were then heated at 140 °C in vacuo (0.1 mbar) for 12 h to ensure complete decomposition and reaction of any diazirine or diazoalkane moieties (formed from isomerization[34]) present after photolysis. The polymers obtained after each stage (photolysis and heating) were analyzed using GPC, NMR, IR, and UV−vis spectroscopic analyses.

Photochemical polymerization of the diazirine monomers **1**−**4** in the bulk and in hexafluorobenzene and perfluoropyridine afforded polyethers as cream to yellow/brown solids in yields ranging from 95 to 99%. Subsequent thermal treatment of the material obtained from the photochemical polymerizations resulted in the formation of polyethers as glassy yellow to brown solids with a reduction in weight of 0−6%. Polyethers constructed using monomers **1**−**3** were found to be partially soluble in tetrahydrofuran (THF) and soluble in methanol, dimethylformamide (DMF), and dimethyl sulfoxide (DMSO). In contrast, polyethers derived from monomer **4** using photolysis were soluble in DMF and DMSO upon heating, whereas those derived from monomer **4** using photolysis followed by thermolysis were insoluble in all organic solvents studied.

GPC analysis of the polyethers (Table 1) obtained after photolysis revealed that the materials molecular weight characteristics were dependent on the type of diazirine monomer and solvent employed. For example, polyethers **P1.1a**−**P1.3a** synthesized from the 3-methyldiazirine monomer **1** possessed considerably lower degree of polymerization (DP) values when compared to polyethers **P2.1a**−**P2.3a** synthesized from the 3-(trifluoromethyl)diazirine monomer **2**. The low molecular weight characteristics of polyethers synthesized from the 3-methyldiazirine monomer **1** can be attributed to the ability of the photogenerated arylmethylcarbenes to participate in intramolecular rearrangements resulting in the formation of styrenic species,[35] which, in turn, competes with the desired O−H insertion reaction. The polymerization process was further

Scheme 3. Synthesis of 3-(Trifluoromethyl)diazirines 22−24: (a) *n*-BuLi, *N*,*N*-diethyltrifluoroacetamide; (b) $NH_2OH{\cdot}HCl$; (c) TsCl, NEt_3, DMAP; (d) NH_3, (e) Ag_2O

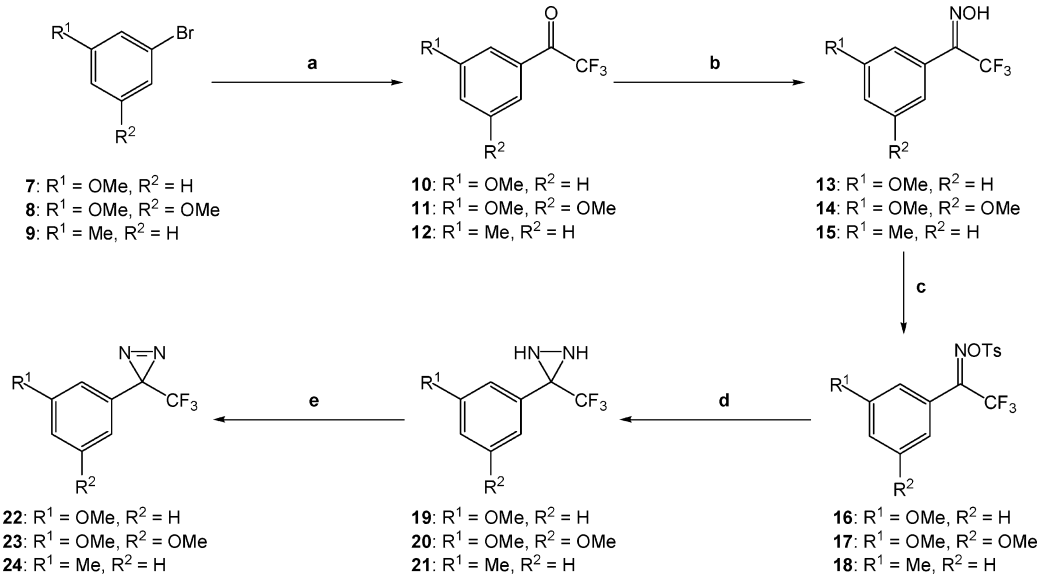

Scheme 4. Synthesis of 3-(3-(Hydroxymethyl)phenyl)-3-(trifluoromethyl)diazirine 4: (a) NBS, 1,1′-Azobis(cyclohexane−carbonitrile); (b) $AgNO_3$, Water/Dioxane

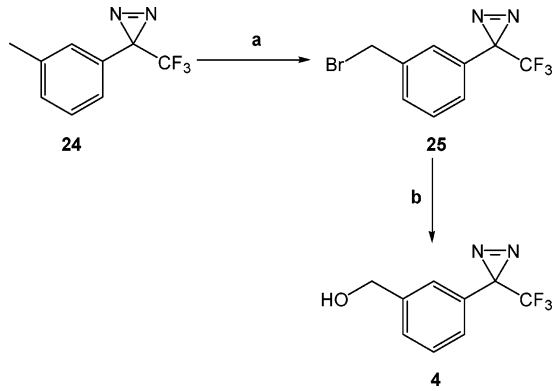

complicated by the tendency of arylcarbenes to react with diazirines and diazoalkanes to afford azines.[36] Photochemical polymerization of the 3-(trifluoromethyl)diazirine monomers **2**−**4** in hexafluorobenzene or perfluoropyridine afforded polyethers with DP values of between 25 and 74. Similarly, photolysis of neat monomers **2** and **4** afforded polyethers **P2.1a** and **P4**.**1a** with DP values of 36 and 45, respectively; however, polymerization of the monomer **3** in the neat phase resulted in the formation of smaller oligomers **P3.1a**. The low molecular weight of **P3.1a** is unsurprising given that at standard temperature and pressure the monomer **3** is a solid, whereas monomers **2** and **4** are oils.

Thermal treatment of the polyethers **P1.1a**−**P4**.**3a** afforded the polyethers **P1.1b**−**P4.3b**, respectively, which were characterized via GPC analysis (Table 2). In all cases thermal treatment of the polyethers resulted in an increase in the molecular weight of the material, while the polydispersity remained comparatively constant. The increase in molecular weight observed between the polyethers and their thermally cured derivatives was attributed to thermal activation of remaining diazirine and diazoalkane moieties present after the photolytic stage of the polymerization process or cross-linking between polymer chains.

The change in molecular weight characteristics of the polyethers with variation of the initial monomer concentration (Table 3) was studied for each of the monomers **1**−**4**. GPC analysis of polyethers **P1.4b**−**P1.4e** revealed an increase in molecular weight with an increase in monomer concentration, with the exception of the **P1.4a**, which only exhibited partial solubility in DMF. The observed increase in molecular weight of the polyethers with increase in monomer concentration is consistent with the extent of intramolecular rearrangement that might be expected at lower concentrations. For example, at low monomer concentrations the carbenes produced are more likely to participate in rearrangements prior to bimolecular reactions, whereas at high monomer concentrations the probability of the carbene interacting with another molecule increases. Unfortunately, the polyethers synthesized from the phenolic monomer **2** at concentrations of <0.25 M were found to be insoluble; thus, it was not possible to accurately determine the effect that the monomer concentration had on the polyethers molecular weight characteristics. GPC analysis of polyethers **P3.4a**−**P3.4e** and **P4.4a**−**P4.4e** revealed an increase in molecular weight with an increase in monomer concentration. It is proposed that the observed trend in molecular weight with monomer concentration arises from the difference in reactivity of singlet- and triplet-state carbenes[37] formed from the diazirine monomers **3** and **4**. For example, at low monomer concentrations the probability of photogenerated singlet carbenes to participate in intersystem crossing processes to the triplet state is high; thus, a higher proportion of the carbenes react from a triplet state, resulting in radical-like intermolecular reactions. At high monomer concentrations it is more likely that the carbenes react rapidly in an intermolecular fashion from a single state, thus resulting in concerted insertion processes. The high efficiency of concerted insertion reactions when compared to radical abstraction, propagation, and dimerization reactions under the experimental condition employed leads to the formation of higher molecular weight species at high monomer concentrations.

The effect of reaction time upon the molecular weight characteristics of the polyethers was investigated using the benzyl alcohol monomer **4**. Identical solutions of the monomer **4** in hexafluorobenzene (0.52 M) were irradiated for set periods of time (5, 10, 15, 20, 30, 40, 60, 90, 150, 300, 600, 1200, and 2400 min) to afford polyethers **P4.5a**−**P4.5l**, respectively. GPC analysis of the polyethers **P4.5a**−**P4.5l** revealed that the molecular weight and PDI of the polyethers increased with an increase in the reaction time (Table 4).

Table 1. Reaction Conditions Employed for the Synthesis of Polyethers P1.1a−P4.3a and Their Molecular Weight Characteristics

polyether	monomer	conditions	solvent	concn/M	M_w[a]/kDa	M_n[a]/kDa	PDI[a]	DP
P1.1a	**1**	*hν*	neat	N/A[b]	1.8	0.9	2.1	15
P1.2a	**1**	*hν*	C_6F_6[c]	0.68	1.6	0.7	2.2	13
P1.3a	**1**	*hν*	C_5F_5N[d]	0.68	1.7	0.8	2.2	14
P2.1a	**2**	*hν*	neat	N/A	6.2	4.2	1.5	36
P2.2a	**2**	*hν*	C_6F_6	0.50	8.1	3.5	2.3	47
P2.3a	**2**	*hν*	C_5F_5N	0.49	11.0	3.7	3.0	63
P3.1a	**3**	*hν*	neat	N/A	0.8	0.5	1.5	4
P3.2a	**3**	*hν*	C_6F_6	0.23	4.8	2.9	1.7	25
P3.3a	**3**	*hν*	C_5F_5N	0.24	6.1	3.0	2.0	32
P4.1a	**4**	*hν*	neat	N/A	8.5	3.6	2.3	45
P4.2a	**4**	*hν*	C_6F_6	0.46	14.3	3.7	3.9	76
P4.3a	**4**	*hν*	C_5F_5N	0.46	13.9	4.0	3.5	74

[a] GPC analysis was conducted in DMF containing 0.05 M LiBr at 60 °C. [b] N/A = not applicable. [c] Hexafluorobenzene. [d] Perfluoropyridine.

Table 2. Reaction Conditions Employed for the Synthesis of Polyethers P1.1b−P3.3b and Their Molecular Weight Characteristics

polyether	monomer	conditions	solvent[a]	concn/M	M_w[b]/kDa	M_n[b]/kDa	PDI[b]	DP
P1.1b	**1**	*hν*/Δ	neat	N/A[c]	2.0	1.0	2.1	17
P1.2b	**1**	*hν*/Δ	C_6F_6[d]	0.68	2.2	1.0	2.3	18
P1.3b	**1**	*hν*/Δ	C_5F_5N[e]	0.68	2.3	1.0	2.2	19
P2.1b	**2**	*hν*/Δ	neat	N/A	10.8	5.9	1.8	62
P2.2b	**2**	*hν*/Δ	C_6F_6	0.50	14.3	5.3	2.7	82
P2.3b	**2**	*hν*/Δ	C_5F_5N	0.49	18.4	6.1	3.0	106
P3.1b	**3**	*hν*/Δ	neat	N/A	3.5	2.1	1.6	18
P3.2b	**3**	*hν*/Δ	C_6F_6	0.23	7.2	3.8	1.9	38
P3.3b	**3**	*hν*/Δ	C_5F_5N	0.24	7.1	4.1	1.8	37

[a] Solvent use in photochemical polymerization stage. [b] GPC analysis was conducted in DMF containing 0.05 M LiBr at 60 °C. [c] N/A = not applicable. [d] Hexafluorobenzene. [e] Perfluoropyridine.

Table 3. Reaction Conditions Employed for the Synthesis of Polyethers P1.4b−P1.4e, P3.4a−P3.4e, and P4.4a−P4.4e and Their Molecular Weight Characteristics

polyether	monomer	conditions	solvent	concn/M	M_w[a]/kDa	M_n[a]/kDa	PDI[a]	DP
P1.4b	**1**	*hν*	C_6F_6[b]	0.17	1.2	0.5	2.2	10
P1.4c	**1**	*hν*	C_6F_6	0.34	1.7	0.6	2.9	14
P1.4d	**1**	*hν*	C_6F_6	0.67	1.8	0.8	2.3	15
P1.4e	**1**	*hν*	C_6F_6	1.31	1.9	0.8	2.3	16
P3.4a	**3**	*hν*	C_5F_5N[c]	0.02	3.4	1.2	2.7	18
P3.4b	**3**	*hν*	C_5F_5N	0.05	4.4	1.3	3.3	23
P3.4c	**3**	*hν*	C_5F_5N	0.09	4.5	1.5	3.0	24
P3.4d	**3**	*hν*	C_5F_5N	0.14	4.9	1.8	2.7	26
P3.4e	**3**	*hν*	C_5F_5N	0.18	5.7	1.8	3.1	30
P4.4a	**4**	*hν*	C_6F_6	0.06	5.1	1.6	3.1	27
P4.4b	**4**	*hν*	C_6F_6	0.12	7.6	1.9	4.1	40
P4.4c	**4**	*hν*	C_6F_6	0.23	11.2	2.2	5.0	60
P4.4d	**4**	*hν*	C_6F_6	0.46	14.4	2.6	5.6	76
P4.4e	**4**	*hν*	C_6F_6	0.92	15.0	2.5	6.1	80

[a] GPC analysis was conducted in DMF containing 0.05 M LiBr at 60 °C. [b] Hexafluorobenzene. [c] Perfluoropyridine.

Table 4. Reaction Conditions Employed for the Synthesis of Polyethers P4.5a−P4.5l and Their Molecular Weight Characteristics

polyether	conditions	solvent	concn/M	time/min	M_w[a]/kDa	M_n[a]/kDa	PDI[a]	DP
P4.5a	*hν*	C_6F_6[b]	0.52	5	0.4	0.3	1.4	2
P4.5b	*hν*	C_6F_6	0.52	10	1.2	0.8	1.4	6
P4.5c	*hν*	C_6F_6	0.52	15	1.7	1.1	1.5	9
P4.5d	*hν*	C_6F_6	0.52	20	3.7	2.4	1.6	20
P4.5e	*hν*	C_6F_6	0.52	30	4.0	2.6	1.6	21
P4.5f	*hν*	C_6F_6	0.52	60	4.3	2.7	1.6	23
P4.5g	*hν*	C_6F_6	0.52	90	4.7	2.9	1.6	25
P4.5h	*hν*	C_6F_6	0.52	150	5.4	3.1	1.7	29
P4.5i	*hν*	C_6F_6	0.52	300	5.8	3.2	1.8	31
P4.5j	*hν*	C_6F_6	0.52	600	9.2	3.3	2.8	49
P4.5k	*hν*	C_6F_6	0.52	1200	13.1	3.5	3.8	70
P4.5l	*hν*	C_6F_6	0.52	2400	16.0	3.2	4.9	85

[a] GPC analysis was conducted in DMF containing 0.05 M LiBr at 60 °C. [b] Hexafluorobenzene.

A plot of molecular weight and PDI vs reaction time (Figure 2) revealed that initially the polymerization process proceeded rapidly as material with a weight-average molecular weight (M_w) value of ca. 4 kDa was obtained after a period of just 30 min. After the first 30 min the polymerization was found to proceed gradually with material possessing M_w values of ca. 8 and 16 kDa being formed after 8 and 40 h, respectively. Similarly, the variation of number-average molecular weight (M_n) with time

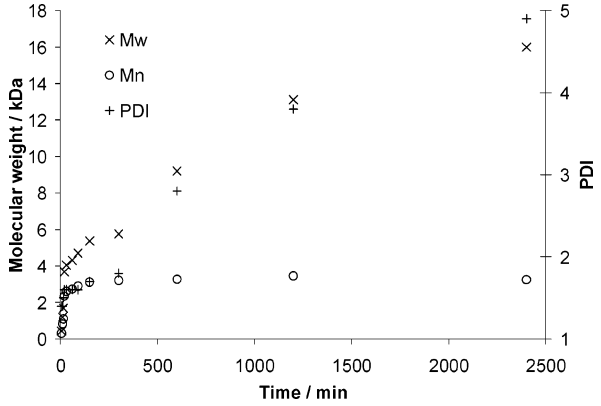

Figure 2. Change in molecular weight characteristics of polyethers with respect to reaction time.

was found to increase rapidly at the outset; however, after 90 min the M_n value remained essentially constant. These results imply that the polymerization process features characteristics common to both chain- and step-growth polymerization approaches.

The change in M_w with time observed for the polymerization of monomer **4** is characteristic of a chain-growth approach, whereas the change in M_n with time leading to an increase in the PDI values is characteristic of a step-growth approach. Therefore, polymerization of monomer **4** can be regarded as a hybrid process incorporating traits common to both chain- and step-growth polymerization approaches. It is proposed that the unusual polymerization pathway observed for monomer **4** occurs for several reasons: (i) At the outset of the polymerization a large proportion of the diazirine moieties are activated, leading to the formation of carbenes and diazoalkanes. The carbenes produced react rapidly, resulting in the formation of large molecules in a very short space of time. (ii) The reactive and unselective nature of carbenes means that they do not have time to diffuse in the mixture before reaction, and thus chain propagation reactions occur at the chain ends and along the backbone of the growing polymer molecules, leading to the formation of hyperbranched materials. (iii) The diazoalkanes present in the reaction mixture are considerably more stable to the photolytic conditions employed than the corresponding diazirines and, therefore, are activated and converted to carbenes at a slower rate. Thus, after all the diazirine has been activated the reaction mixture consists of polymeric materials that possess predominantly diazoalkane functionalities. Over longer periods of irradiation the diazoalkane moieties are converted to carbenes, which can then insert into other polymeric chains, resulting in a gradual increase of M_w with time.

IR and UV−vis spectroscopic analysis of the polyethers **P1.1a**−**P4.3a** and their thermally cured derivatives revealed very similar spectra and changes in the structure of the polyethers occurring after thermal treatment were not detected. The absence of absorptions in the range 2000−2100 cm^{-1} indicated that diazoalkane residues were not in evidence after photolytic or thermal treatment of the monomers **1**−**4**. IR spectroscopic analysis of polyethers **P1.1a**−**P1.3a** revealed several absorptions at ca. 3330, 2980, 1600, and 1250 cm^{-1}, corresponding to O−H, C−H, aromatic C−C, and C−O bonds, respectively. Similarly, IR spectra of polyethers **P2.1a**−**P4.3a** featured absorptions at ca. 3330, 1600, and 1250 cm^{-1}, corresponding to O−H, aromatic C−C, and C−O bonds, respectively. In addition, strong absorptions at ca. 1160 cm^{-1} corresponding to C−F bonds were also present. The IR spectra obtained for the polymers are consistent with a polyether-type structure, in which the alcoholic

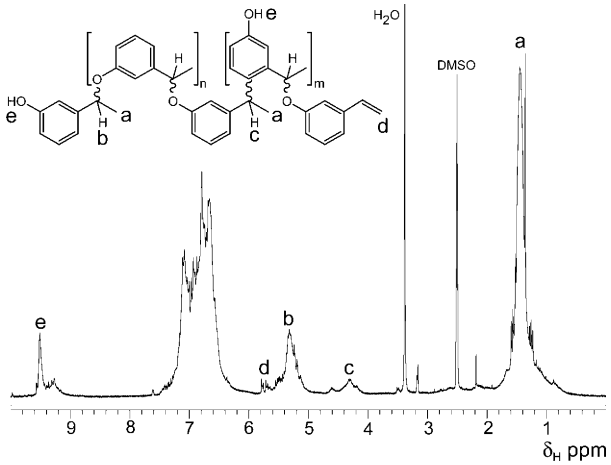

Figure 3. ^{1}H NMR spectrum (d_6-DMSO) of polyether **P1.2a**.

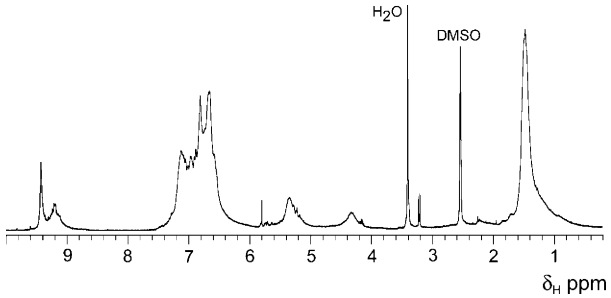

Figure 4. ^{1}H NMR spectrum (d_6-DMSO) of polyether **P1.2b**.

functionalities are hydrogen bonded. UV−vis spectroscopic analysis of the polyethers consisted of absorption bands at 210 and 257−280 nm, corresponding to the aromatic groups. The absence of absorption bands in the range 350−380 nm indicated that all the diazirine had decomposed under the conditions employed, with the exception of the UV−vis spectrum of polyether **P3.1a**, which featured a weak absorption at 356 nm, implying that trace quantities of these reactive moieties remained.

^{1}H NMR spectroscopic analysis of the polyethers **P1.1a**−**P1.3a** revealed several broad multiplets consistent with a polyether-type structure. For example, the ^{1}H NMR spectrum of polyether **P1.2a** (Figure 3) consists of multiplet resonances at ca. δ_H 1.4, 5.3, and 6.9 ppm, corresponding to methyl, methine, and aromatic protons of the desired polyether, respectively. The formation of the ether linkage was also indicated by ^{13}C NMR spectroscopic analysis, which revealed several resonances at ca. δ_C 160 ppm, corresponding to aromatic carbons adjacent to alkoxy groups.

A broad resonance observed at δ_H 4.3 ppm in ^{1}H NMR spectra was assigned to methine protons adjacent to two aromatic groups, such as those formed via alkylation of carbocations[38] with the *ortho* and *para* aromatic carbons of phenolic molecules.[39] A double-doublet resonance at δ_H 5.7 ppm is characteristic of a geminal proton of styrene and as a result was assigned to styrenic end groups present in the polymer. In addition, broad multiplets at ca. δ_H 9.3 and 9.5 ppm were also observed that corresponded to the proton resonances of phenolic groups in deuterated DMSO (δ_H 9.60 ppm) and thus were assigned to phenolic alcohol chain ends within the polymeric structure. ^{1}H NMR spectroscopic analysis of the thermally cured polyether **P1.2b** (Figure 4) revealed resonances at identical chemical shifts to those observed for its precursor **P1.2a**, although the majority of resonances were less well resolved.

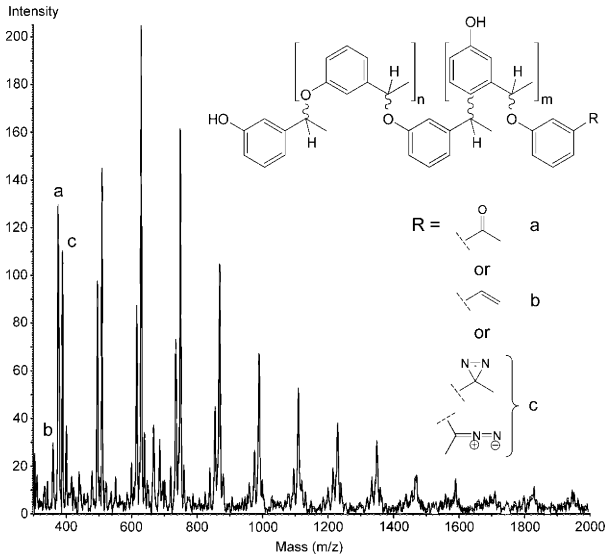

Figure 5. MALDI-ToF mass spectrometric analysis of polyether **P1.1b** consisting of several series of peaks originating from polymer chains with different end-group functionalization.

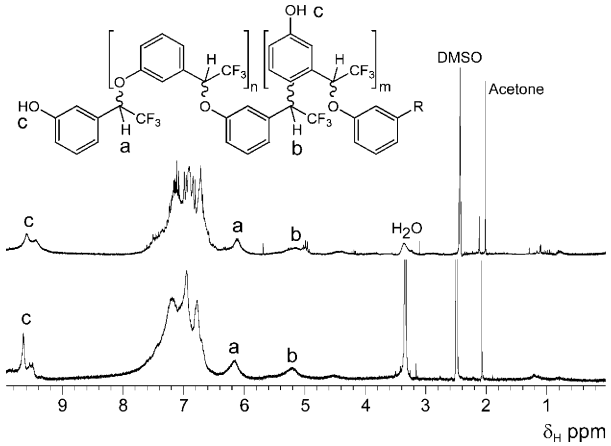

Figure 6. ^{1}H NMR spectra (d_6-DMSO) of polyethers **P2.3a** produced via photochemical polymerization (top) and **P2.3b** post-thermal treatment (bottom).

The NMR spectroscopic data of the polyethers **P1.1a**−**P1.3a** and **P1.1b**−**P1.3b** indicated that these polymers are disperse not only in terms of molecular weight characteristics but also via the different covalent linkages found, thus leading ultimately to hyperbranched architectures. The majority of the material produced was composed of the desired ether linkages, with a small proportion of 1,1-diphenylethane-type linkages resulting in branch points and hydroxyl functionalities throughout the polymer backbone. The end-group functionality present in polyether **P1.1b** was determined by MALDI-ToF mass spectrometric analysis (Figure 5), which revealed several series of peaks with a repeat pattern every 120 *m*/*z* corresponding to the monomer unit and a combination of styrene, ketone,[40] and diazirine/diazoalkane terminal groups. Unfortunately, MALDI-ToF mass spectrometric analysis of the fluorinated polyethers synthesized from monomers **2**, **3**, and **4** was unsuccessful.

^{1}H NMR spectroscopic analysis of the polyethers **P2.1a**−**P2.3a** (for example, Figure 6) revealed broad resonances at ca. δ_H 5.2, 6.2, 7.0, and 9.6 ppm, corresponding to methine protons adjacent to two aromatic substituents, methine protons adjacent to a phenolic oxygen, aromatic protons, and hydroxyl protons, respectively. The thermally treated polyethers **P2.1b**−**P2.3b** were found to possess similar ^{1}H NMR spectra to their precursors **P2.1a**−**P2.3a**, respectively, although broadening of the resonances was observed.

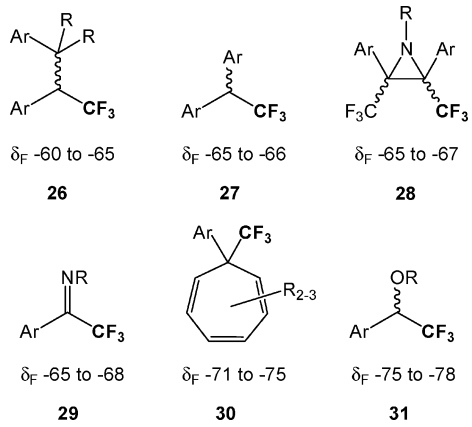

Figure 7. Structures of predicted linkages and the approximate ^{19}F NMR trifluoromethyl group chemical shift values in $CDCl_3$.

^{1}H NMR spectroscopic analysis of the polyethers **P3.1a**−**P3.3a** and their thermally cured derivatives **P3.1b**−**P3.3b**, respectively, revealed multiplet resonances between δ_H 5.1−5.6, 5.8−7.0, and 8.8−10.0 ppm, corresponding to methine protons adjacent to two aromatic substituents and methine protons adjacent to a phenolic oxygen combined with aromatic protons and hydroxyl protons, respectively. The low molecular weight of the polyether **P3.1a** obtained from bulk reaction was also indicated by ^{1}H NMR spectroscopic analysis, which revealed well-defined resonances that are indicative of the presence of small oligomers. However, ^{1}H NMR spectroscopic analysis of the thermally treated derivative **P3.1b** was more consistent with the analysis obtained for the polyethers **P3.2a** and **P3.3a** and implied that photolytic decomposition of the diazirinyl moieties in **P3.1a** was incomplete. ^{1}H NMR spectroscopic analysis of the polyethers **P4.1a**−**P4.3a** revealed broad resonances at ca. δ_H 4.5, 5.3, and 7.4 ppm. The resonance at ca. δ_H 4.5 ppm was comprised of two overlapping resonances corresponding to methylene protons and methine protons adjacent to alkyl groups. Resonances observed at δ_H 5.3 and 7.4 ppm corresponded to methine protons adjacent to alkoxy groups and aromatic protons, respectively.

The presence of trifluoromethyl groups throughout the architecture of polyethers synthesized from 3-(trifluoromethyl)-diazirine monomers **2**−**4** enabled ^{19}F NMR spectroscopic analysis to be employed to determine and quantify the various types of linkages formed in the polymerization process. To assist the determination of the structure of polymers synthesized from 3-(trifluoromethyl)diazirine monomers, a database of ^{19}F NMR shifts and coupling constants based on previously synthesized compounds was compiled.[41] Use of this spectroscopic data enabled the prediction of the different types of linkages that maybe formed during the polymerization of the monomers **2**−**4** and thus the variety of ^{19}F NMR resonances expected for trifluoromethyl groups adjacent to those linkages (Figure 7). It should be noted that the chemical shift values of ^{19}F nuclei resonances of the trifluoromethyl groups were subject to subtle changes in the chemical shift values when the analyses were conducted in different solvents. For example, the ^{19}F NMR chemical shift values for trifluoroacetophenone and trifluoroacetophenone azine groups in $CDCl_3$ were observed at δ_F −72.1 and −67.6 ppm, whereas in d_6-DMSO these resonances were evident downfield at δ_F −71.5 and −66.8 ppm, respectively.

^{19}F NMR spectroscopic analysis of the polyethers **P2.2a** and **P2.2b** (Figure 8) revealed four major sets of resonances ranging

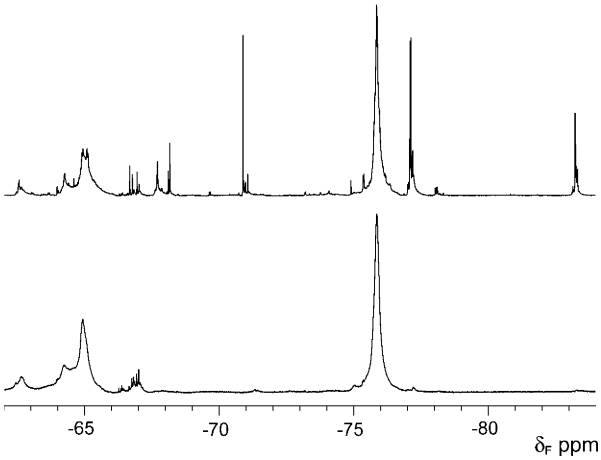

Figure 8. ^{19}F NMR spectra (d_6-DMSO) of polyethers **P2.2a** produced via photochemical polymerization (top) and **P2.2b** post-thermal treatment (bottom).

from δ_F −62 to −63, −64 to −65, −66 to −68, and −75 to −77 ppm, which were assigned to trifluoromethyl groups in the environments provided by linkages **26**, **27**, **28**/**29**, and **31**, respectively. The presence of low-intensity resonances at ca. δ_F −71 and −83 ppm in the ^{19}F NMR spectrum of polyether **P2.2a** could not be determined; however, upon thermal treatment these resonances were not observed, thus implying that they arose from trifluoromethyl groups adjacent to thermally unstable linkages/groups. The inclusion of 1,1-diphenylethane linkages (**27**) in the polyethers gives rise to hydroxyl functionalities and thus branch points along the polymer backbone, ultimately resulting in hyperbranched architectures. In common with studies of other hyperbranched polymers reported in the literature,[42] the degree of branching of these polymers proved difficult to ascertain given the structural diversity of the linear and branching units within the polyether architecture.

As a result of integration of the groups of resonances observed in the ^{19}F NMR spectra of the polyethers **P2.1a**−**P4**.3a and **P2.1b**−**P3.3b**, it was possible to estimate the percentage of the different types of linkage from which the polymers were comprised (Table 5). For example, integration of the ^{19}F NMR spectra obtained for polyether **P2.2a** (Figure 8) revealed that it contained linkages **26**, **27**, **28**/**29**, and **31** in relative amounts of 3, 28, 2, and 55%, respectively. It was evident from ^{19}F NMR spectroscopic analysis that the most abundant linkage type in the polyethers was the desired ether linkage **31** (37−81%) formed via carbene insertion into alcoholic O−H bonds. Generally, the relative amounts of the ether linkage **31** in polyethers **P2.1b**−**P2.3b** and **P3.2b**−**P3.3b** obtained by thermal treatment were similar to the amount observed in their precursors, **P2.1a**−**P2.3a** and **P3.2a**−**P3.3a**. An exception to this observation was the polyether **P3.1a**. Thermal treatment of the polyether **P3.1a** to yield the polyether **P3.1b** was accompanied by an increase in the relative amounts of the ether linkage **31** from 37 to 61%. The increase in ether linkage **31** observed upon thermal treatment results from activation of diazirine moieties still present after the initial photochemical polymerization.

The second most abundant type of linkage in polyethers **P2.1a**−**P3.3a** and **P2.1b**−**P3.3b** was the 1,1-diphenylethane linkage **27** (5−36%) formed via the production of cationic species capable of alkylating phenolic derivatives. However, the relative amounts of 1,1-diphenylethane linkage present in the polyethers synthesized from the monomer **2** (20−36%) was considerably more than that observed for the polyethers synthesized from the monomer **3** (5−12%). The observed difference can be explained by consideration of the steric interactions caused by aromatic substituents. For example, the monomer **2** consists of a central benzene core complete with two substituents at the *C*-1 and *C*-3 positions; thus, alkylation at the *C*-4 or *C*-6 position (relative to the hydroxy substituent) was favored. In contrast, the monomer **3** consists of a central benzene core complete with three substituents at the *C*-1, *C*-3, and *C*-5 positions; thus, alkylation at the *C*-2, *C*-4, or *C*-6 position (relative to the hydroxy substituent) led to a large increase in steric congestion around the benzene unit and was, therefore, disfavored. ^{19}F NMR spectroscopic analysis of the polyether **P3.1a** revealed a singlet resonance at δ_F −65 ppm that accounted for ca. 20% of the total resonances and corresponded to trifluoromethyl groups adjacent to diazirine moieties, thus confirming that photolysis of **3** in the neat phase for 24 h was insufficient for the total activation of the diazirine functionality. The increase in molecular weight (Table 2) of the thermally cured derivative **P3.1b** (compared to **P3.1a**) can be rationalized by thermal activation of the unreacted diazirine moieties to afford ether linkages as indicated by ^{19}F NMR spectroscopic analysis, which revealed the disappearance of the trifluoromethyl group resonance corresponding to the diazirine moieties and an increase in the resonances of trifluoromethyl groups adjacent to ether linkages. ^{19}F NMR spectroscopic analysis of the polyethers **P4.1a**−**P4.3a** revealed four major resonances at ca. δ_F −64, −67, −74, and −76 ppm, corresponding to trifluoromethyl groups adjacent to linkages **26**, **28**/**29**, **30**, and **31**, respectively. ^{19}F NMR spectroscopic analysis of the polyether **P4.2a** revealed that its structure consisted predominantly of ether linkages **31** (72%), alkyl linkages **26** (17%), and aziridine **28** and azine linkages **29** (7%). The presence of alkyl linkages in the polyether structure affords branching units, and thus the polymers synthesized from monomer **4** are also hyperbranched in nature.

Conclusions

This study has shown that it is possible to generate functionalized hyperbranched polyethers via carbenes photogenerated from diazirines that feature either phenolic or benzyl alcohol moieties. Detailed spectroscopic analysis revealed that the hyperbranched polyethers featured a range of polymeric linkages that arose from carbene insertion into the desired O−H bonds and C-alkylation processes. In all of the polyethers thus produced, the desired carbene insertion process was predominant. Further studies to explore the general applicability of this polymerization method are currently under investigation.

Experimental Section

Synthesis of 3-(3-Hydroxyphenyl)-3-methyldiazirine 1. 3-Methyl-3-(3-(tetrahydro-2*H*-pyran-2-yloxy)phenyl)diazirine **6** (9.13 g, 39.4 mmol) and hydroxylamine hydrochloride (5 mol %, 0.135 g, 1.95 mmol) were dissolved in ethanol (120 mL), and the mixture was stirred under argon in the dark for 18 h. The mixture was concentrated in vacuo, and the resulting residue was dissolved in diethyl ether (200 mL). The organic solution was washed with water (2 × 150 mL), dried ($MgSO_4$), filtered, and concentrated in vacuo to afford a pale pink oil. Purification via column chromatography (3:1 hexane:diethyl ether) afforded 3-(3-hydroxyphenyl)-3-methyldiazirine **1** as a white solid, 5.30 g (92%); mp 44−45 °C. ^{1}H NMR (250 MHz, $CDCl_3$, TMS): δ_H 1.49 (*s*, 3H, C**H**$_3$), 4.95 (*s*, 1H, O**H**), 6.36−6.36 (*m*, 1H, Ar**H**), 6.48−6.52 (*m*, 1H, Ar**H**), 6.74−6.78 (*m*, 1H, Ar**H**), 7.20 (*t*, J = 7.9 Hz, 1H, Ar**H**) ppm. ^{13}C NMR (62.5 MHz, $CDCl_3$): δ_C 18.0 (**C**H$_3$), 26.5 (**C**N$_2$), 113.0 (Ar**C**H), 114.9 (Ar**C**H), 118.5 (Ar**C**H), 129.9 (Ar**C**H), 142.2 (Ar**C**C), 156.0 (Ar**C**O) ppm. IR υ_{max}/cm^{-1} (thin film): 1208, 1307, 1388, 1453, 1585, 1605, 3352. UV−vis (MeOH): λ = 374.2 (N=

Table 5. Relative Percentages of Covalent Linkage Types 26, 27, 28/29, 30, and 31 Present in the Polyethers P2.1a−P4.3a and P2.1b−P3.3b

			linkage/%[a]					
polymer	conditions	solvent	**26**[b]	**27**[b]	**28**[b]/**29**[b]	**30**[b]	**31**[b]	unidentified[c]
P2.1a	*hν*	neat	0	31	14	0	55	0
P2.1b	*hν*/Δ	neat	0	34	10	0	56	0
P2.2a	*hν*	C_6F_6[d]	3	28	2	0	55	12
P2.2b	*hν*/Δ	C_6F_6[e]	6	41	3	0	50	0
P2.3a	*hν*	C_5F_5N	2	20	1	0	69	8
P2.3b	*hν*/Δ	C_5F_5N	4	32	3	0	60	7
P3.1a	*hν*	neat	2	4	30	0	37	27[g]
P3.1b	*hν*/Δ	neat	5	5	18	0	61	11
P3.2a	*hν*	C_6F_6	3	7	5	0	68	17
P3.2b	*hν*/Δ	C_6F_6	3	10	5	0	72	10
P3.3a	*hν*	C_5F_5N	6	12	6	0	72	4
P3.3b	*hν*/Δ	C_5F_5N	5	12	5	0	73	5
P4.1a	*hν*	neat	15	N/A[f]	20	5	54	6
P4.2a	*hν*	C_6F_6	17	N/A	7	1	72	3
P4.3a	*hν*	C_5F_5N	8	N/A	7	1	81	3

[a] Relative amount of linkage compared to sum of all linkages as determined from ^{19}F NMR spectroscopic analysis. [b] See Figure 6 for linkage structures. [c] Resonances that could not be assigned to linkage types. [d] Hexafluorobenzene. [e] Perfluoropyridine. [f] N/A = not applicable. [g] Predominantly diazirine.

N) nm. CI-MS ($[M]^+-N_2$) calculated for C_8H_8O: 120.0575; found: 120.0575. Anal. Calcd for $C_8H_8N_2O$: C, 64.85; H, 5.44; N, 18.90. Found: C, 64.96; H, 5.57; N, 18.92.

Synthesis of 3-(3,5-Dihydroxylphenyl)-3-(trifluoromethyl)-diazirine 3.[43] 3-(Trifluoromethyl)-3-(3,5-dimethoxyphenyl)diazirine **23** (9.61 g, 39.0 mmol) was dissolved in anhydrous dichloromethane (180 mL). Boron tribromide (10.9 g, 115 mmol) was added dropwise over 30 min, and the mixture was stirred in the dark under argon for 32 h. Water (30 mL) was added carefully followed by dichloromethane (100 mL) and water (200 mL). After 1 h the organic phase was removed, and the aqueous phase washed with diethyl ether (5 × 100 mL). The combined organic extracts were dried ($MgSO_4$), filtered, and concentrated in vacuo at 40 °C to afford a pale yellow solid. Purification via column chromatography (1:1 hexane:diethyl ether) afforded 3-(3,5-dihydroxylphenyl)-3-(trifluoromethyl)diazirine **3** as a white crystalline solid, 8.30 g (97%); T_d = 112 °C. ^1H NMR (250 MHz, d_6-DMSO): δ_H 6.02−6.03 (*m*, 2H, 2Ar**H**), 6.34 (*t*, *J* = 2.1 Hz, 1H, Ar**H**), 9.76 (*s*, 2H, 2O**H**) ppm; ^{13}C NMR (62.5 MHz, $CDCl_3$) δ_C 29.8 (*q*, *J* = 40.0 Hz, **C**N_2), 105.5 (Ar**C**H), 106.1 (2Ar**C**H), 124.0 (*q*, *J* = 273.8 Hz, **C**F_3), 132.4 (Ar**C**C), 160.9 (2Ar**C**O) ppm. ^{19}F NMR (235 MHz, CD_3OD, $CFCl_3$): δ_F −63.1 (*s*, C**F**$_3$) ppm. IR υ_{max}/cm^{-1} (thin film): 1151, 1201, 1296, 1508, 1541, 1601, 1617, 3335. UV−vis (MeOH): λ = 356.6 (N═N) nm. CI-MS ($[M]^+$) calculated for $C_8H_5F_3N_2O_2$: 218.0303; found: 218.0300. Anal. Calcd for $C_8H_5F_3N_2O_2$: C, 44.05; H, 2.31; N, 12.84. Found: C, 43.94; H, 2.38; N, 12.17.

Synthesis of 3-(3-(Hydroxymethyl)phenyl)-3-(trifluoromethyl)diazirine 4. 3-(Trifluoromethyl)-3-(3-methylphenyl)diazirine **24** (2.80 g, 14.0 mmol) and NBS (2.49 g, 14.0 mmol) were dissolved in anhydrous dichloromethane (50 mL) under argon and heated to and maintained under reflux. A solution of 1,1′-azobis(cyclohexane−carbonitrile) (2.5 mol %, 70.0 mg, 0.287 mmol) in anhydrous dichloromethane (1 mL) was added, and the mixture was heated at 80 °C for 48 h. After cooling to room temperature the mixture was added to saturated sodium thiosulfate (250 mL) and stirred for 2 h. The resulting solution was then extracted with dichloromethane (4 × 70 mL). The combined organic extracts were dried ($MgSO_4$), filtered, and concentrated in vacuo to afford the crude benzyl bromide, 3-(3-(bromomethyl)phenyl)-3-(trifluoromethyl)diazirine **25**, as a pale orange oil. ^1H NMR (250 MHz, $CDCl_3$, TMS): δ_H 4.38 (*s*, 2H, C**H**$_2$Br), 7.07−7.10 (*m*, 2H, 2Ar**H**), 7.30−7.40 (*m*, 2H, 2Ar**H**) ppm. ^{13}C NMR (62.5 MHz, $CDCl_3$): δ_C 28.7 (*q*, *J* = 40.5 Hz, **C**N_2), 32.6 (**C**H$_2$Br), 122.4 (*q*, *J* = 274.8 Hz, **C**F_3), 126.9 (Ar**C**H), 127.3 (Ar**C**H), 129.8 (Ar**C**H), 130.2 (Ar**C**C), 130.7 (Ar**C**H), 139.2 (Ar**C**C) ppm. ^{19}F NMR (235 MHz, $CDCl_3$, $CFCl_3$): δ_F −65.6 (*s*, C**F**$_3$) ppm. IR υ_{max}/cm^{-1} (thin film): 1157, 1198, 1253, 1343, 1493, 1608 (N═N), 2926. UV−vis (MeOH): λ = 352.8 (N═N) nm. CI-MS ($[M]^+-N_2$) calculated for $C_9H_6BrF_3$: 249.9605; found: 249.9604. The oil was dissolved in a solution consisting of water (40 mL) and dioxane (40 mL), and $AgNO_3$ (3.57 g, 21.0 mmol) was added. The mixture was stirred in the dark for 24 h and then filtered through a pad of Celite. The filtrate was concentrated in vacuo, and the resulting residue was purified via column chromatography (4:1 hexane:dichloromethane) to afford 3-(3-(hydroxymethyl)phenyl)-3-(trifluoromethyl)diazirine **4** as a clear oil, 2.14 g (71%). ^1H NMR (250 MHz, $CDCl_3$, TMS): δ_H 1.82 (*t*, *J* = 5.7 Hz, 1H, O**H**), 4.71 (*d*, *J* = 5.7 Hz, 2H, C**H**$_2$), 7.14−7.17 (*m*, 2H, 2Ar**H**), 7.39−7.45 (*m*, 2H, 2Ar**H**) ppm. ^{13}C NMR (62.5 MHz, $CDCl_3$): δ_C 28.8 (*q*, *J* = 40.4 Hz, **C**N_2), 64.7 (O**C**H$_2$), 122.5 (*q*, *J* = 274.6 Hz, **C**F_3), 125.0 (Ar**C**H), 126.0 (Ar**C**H), 128.4 (Ar**C**H), 129.4 (Ar**C**H), 129.7 (Ar**C**C), 142.1 (Ar**C**C) ppm. ^{19}F NMR (235 MHz, $CDCl_3$, $CFCl_3$): δ_F −65.6 (*s*, C**F**$_3$) ppm. IR υ_{max}/cm^{-1} (thin film): 1046, 1153, 1198, 1249, 1340, 1439, 1609, 2879, 3324. UV−vis (MeOH): λ = 356.1 (N═N) nm. CI-MS ($[M]^+-N_2$) calculated for $C_9H_7F_3O$: 188.0449; found: 188.0440. Anal. Calcd for $C_9H_7F_3N_2O$: C, 50.01; H, 3.26; N, 12.95. Found: C, 49.69; H, 3.34; N, 13.13.

Synthesis of 3-Methyl-3-(3-(tetrahydro-2*H*-pyran-2-yloxy)-phenyl)diazirine 6. 1-[3-(Tetrahydropyran-2-yloxy)-phenyl]ethanone **5** (7.01 g, 31.9 mmol), benzylamine (3.50 mL, 32.1 mmol), and $ZnCl_2$ (2 mol %, 88.1 mg, 0.646 mmol) were added to toluene (120 mL) and heated under reflux using a Dean−Stark trap. After 36 h the mixture was cooled and filtered through Celite, and the filtrate was concentrated in vacuo to afford the crude imine, phenyl-*N*-(1-(3-(tetrahydro-2*H*-pyran-2-yloxy)phenyl)ethylidene)methanamine. ^1H NMR (250 MHz, $CDCl_3$, TMS): δ_H 1.50−1.60 (*m*, 3H, C**H**$_2$ + C**H**H), 1.76−1.82 (*m*, 2H, 2C**H**H), 1.85−1.99 (*m*, 1H, C**H**H), 2.23 (*s*, 3H, C**H**$_3$), 3.50−3.55 (*m*, 1H, C**H**H), 3.78−3.85 (*m*, 1H, C**H**H), 4.65 (*s*, 2H, C**H**$_2$), 5.39 (*t*, *J* = 3.2, 1H, OC**H**), 7.04−7.49 (*m*, 9H, 9Ar**H**) ppm. ^{13}C NMR (62.5 MHz, $CDCl_3$): δ_C 16.4 (**C**H$_3$), 19.2 (**C**H$_2$), 25.6 (**C**H$_2$), 30.8 (**C**H$_2$), 56.1 (N**C**H$_2$), 62.5 (O**C**H$_2$), 96.8 (O**C**H), 115.6 (Ar**C**H), 117.9 (Ar**C**H), 120.6 (Ar**C**H), 125.7 (Ar**C**C), 127.5 (Ar**C**H), 128.1 (2Ar**C**H), 128.8 (2Ar**C**H), 129.5 (Ar**C**H), 140.9 (Ar**C**C), 157.5 (Ar**C**O), 166.3 (**C**═O) ppm. IR υ_{max}/cm^{-1} (thin film): 969, 1037, 1112, 1200, 1285, 1440, 1578, 1634, 1686, 2944. CI-MS ($[M + H]^+$) calculated for $C_{20}H_{23}NO_2$: 310.1807; found: 310.1817. The crude imine was dissolved in dichloromethane (50 mL) and added dropwise over a period of 30 min to liquid ammonia (200 mL) at −78 °C under argon. The mixture was stirred vigorously for 6 h, and then a solution of hydroxylamine-*O*-sulfonic acid (5.42 g, 48.0 mmol) in methanol (50 mL) was added over a period of 30 min. After a further 12 h the mixture was allowed to warm to room temperature; water (150 mL) and dichloromethane (100 mL) were then added. The organic phase was removed, and the aqueous phase was extracted with dichloromethane (4 × 100 mL). The combined organic extracts were dried ($MgSO_4$), filtered, and concentrated in vacuo to afford a yellow oil, which was dissolved in methanol (200 mL) in the dark. Triethylamine (13.5 mL, 96.0 mmol) was added followed by gradual addition of iodine pellets until the intense color

of iodine remained. The mixture was stirred for 2 h and concentrated in vacuo, and the residue was dissolved in diethyl ether (200 mL), which was then added to saturated sodium thiosulfate (100 mL) and stirred for 1 h. The organic phase was removed, washed with water (3 × 100 mL), dried ($MgSO_4$), filtered, and concentrated in vacuo to afford an orange oil. Purification via column chromatography (3:2 dichloromethane:hexane) afforded 3-methyl-3-(3-(tetrahydro-2*H*-pyran-2-yloxy)phenyl)diazirine **6** as a pale yellow oil, 4.84 g (56%). ^{1}H NMR (250 MHz, $CDCl_3$, TMS): δ_H 1.50 (*s*, 3H, C**H**$_3$), 1.56−1.72 (*m*, 3H, C**H**$_2$ + C**H**H), 1.76−1.87 (*m*, 2H, 2C**H**H), 1.90−2.07 (*m*, 1H, C**H**H), 3.55−3.64 (*m*, 1H, OC**H**H), 3.83−3.92 (*m*, 1H, OC**H**H), 5.41 (*m*, 1H, OC**H**), 6.49−6.54 (*m*, 1H, 1Ar**H**), 6.61−6.62 (*m*, 1H, 1Ar**H**), 6.97−7.02 (*m*, 1H, 1Ar**H**), 7.24 (*t*, *J* = 8.0 Hz, 1H, 1Ar**H**) ppm. ^{13}C NMR (62.5 MHz, $CDCl_3$): δ_C 18.0 (**C**H$_3$), 20.1 (**C**H$_2$), 25.8 (**C**H$_2$), 26.6 (**C**N$_2$), 31.2 (**C**H$_2$), 62.9 (O**C**H$_2$), 99.2 (O**C**H), 113.0 (Ar**C**H), 114.9 (Ar**C**H), 118.3 (Ar**C**H), 130.0 (Ar**C**H), 141.7 (Ar**C**C), 156.2 (Ar**C**O) ppm. IR υ_{max}/cm^{-1} (thin film): 1036, 1073, 1125, 1202, 1305, 1455, 1489, 1583, 1601, 2946. UV−vis (MeOH): λ = 373.9 (N═N) nm. CI-MS ([M]$^+$−N$_2$) calculated for $C_{13}H_{16}O_2$: 204.1150; found: 204.1154.

Synthesis of 2,2,2-Trifluoro-1-(3,5-dimethoxyphenyl)ethanone 11. 1-Bromo-3,5-dimethoxybenzene (9.99 g, 46.0 mmol) was dissolved in anhydrous THF (150 mL) and cooled to −78 °C under argon. 1.6 M *n*-butyl lithium in hexanes (28.7 mL, 46.0 mmol) was added over a period of 5 min, and the mixture was stirred for a further 5 min. *N*,*N*-Diethyltrifluoroacetamide (7.77 g, 46.0 mmol) was then added over a period of 5 min, and the mixture was stirred for 2 h. The mixture was then poured into a saturated NH_4Cl (300 mL) solution and stirred rapidly for an hour before extraction with diethyl ether (4 × 150 mL). The combined organic extracts were dried ($MgSO_4$), filtered, and concentrated in vacuo, and the resulting residue was purified via column chromatography (7:3 hexane: dichloromethane) to afford the 2,2,2-trifluoro-1-(3,5-dimethoxyphenyl)ethanone **11** as a crystalline solid, 9.91 g (92%); mp 27−28 °C. ^{1}H NMR (250 MHz, $CDCl_3$, TMS): δ_H 3.85 (*s*, 6H, 2OC**H**$_3$), 6.77 (*t*, *J* = 2.3 Hz, 1H, Ar**H**), 7.19 (*m*, 2H, 2Ar**H**) ppm. ^{13}C NMR (62.5 MHz, $CDCl_3$): δ_C 56.1 (2O**C**H$_3$), 107.8 (Ar**C**H), 108.4 (2Ar**C**H), 117.0 (*q*, *J* = 291.3 Hz, **C**F$_3$), 131.8 (Ar**C**C), 161.4 (2Ar**C**O), 180.7 (*q*, *J* = 34.9 Hz, **C**O) ppm. ^{19}F NMR (235 MHz, $CDCl_3$): δ_F −71.5 (*s*, C**F**$_3$) ppm. IR υ_{max}/cm^{-1} (thin film): 1004, 1069, 1159, 1210, 1284, 1348, 1462, 1593, 1716, 2944. CI-MS ([M]$^+$) calculated for $C_{10}H_9F_3O_3$: 234.0504; found: 234.0505.

Synthesis of 2,2,2-Trifluoro-1-(3,5-dimethoxyphenyl)ethanone oxime 14. 2,2,2-Trifluoro-1-(3,5-dimethoxyphenyl)ethanone **11** (9.60 g, 41.0 mmol) and hydroxylamine hydrochloride (5.70 g, 82.0 mmol) were dissolved in ethanol (200 mL) and heated under reflux for 2 h. The mixture was neutralized with 4 M NaOH, maintained under reflux for a further 2 h, and then stirred at room temperature for 8 h. The mixture was concentrated in vacuo, and the resulting residue was dissolved in water (250 mL) and extracted with diethyl ether (5 × 100 mL). The combined organic extracts were washed with 0.25 M HCl (200 mL) and water (200 mL), dried ($MgSO_4$), filtered, and concentrated in vacuo to afford 2,2,2-trifluoro-1-(3,5-dimethoxyphenyl) ethanone oxime **14** as a white solid, 9.70 g (95%); mp 105−106 °C. ^{1}H NMR (250 MHz, $CDCl_3$, TMS): δ_H 3.82 (*s*, 6H, 2OC**H**$_3$), 6.57 (*t*, *J* = 2.1 Hz, 1H, Ar**H**), 6.61 (*d*, *J* = 2.1 Hz, 2H, 2Ar**H**), 8.65 (*br s*, 1H, O**H**) ppm. ^{13}C NMR (62.5 MHz, $CDCl_3$): δ_C 55.9 (2O**C**H$_3$), 103.0 (Ar**C**H), 107.0 (2Ar**C**H), 120.8 (*q*, *J* = 275.2 Hz, **C**F$_3$), 127.8 (Ar**C**C), 148.0 (*q*, *J* = 32.6 Hz, **C**O), 161.2 (2Ar**C**O) ppm. ^{19}F NMR (235 MHz, $CDCl_3$): δ_F −67.4 (*s*, C**F**$_3$) ppm. IR υ_{max}/cm^{-1} (thin film): 974, 1127, 1157, 1212, 1426, 1461, 1595, 3357. CI-MS ([M]$^+$) calculated for $C_{10}H_{10}F_3NO_3$: 249.0613; found: 249.0605.

Synthesis of *O*-Tosyl-2,2,2-Trifluoro-1-(3,5-dimethoxyphenyl)-ethanone oxime 17. 2,2,2-Trifluoro-1-(3,5-dimethoxyphenyl)ethanone oxime **14** (9.70 g, 38.9 mmol), triethylamine (8.20 mL, 58.4 mmol), *p*-(*N*,*N*-dimethylamino)pyridine (DMAP) (96.1 mg, 0.788 mmol), and *p*-toluenesulfonyl chloride (TsCl) (7.42 g, 38.9 mmol) were dissolved in anhydrous dichloromethane (150 mL) in the dark under argon. After stirring for 12 h, the resulting mixture was washed with 0.25 M HCl (2 × 200 mL), saturated $NaHCO_3$ (2 × 200 mL), and water (200 mL), dried ($MgSO_4$), filtered, and concentrated in vacuo to afford *O*-tosyl-2,2,2-trifluoro-1-(3,5-dimethoxyphenyl)ethanone oxime **17** as a white solid, 15.4 g (98%); mp 113−114 °C. ^{1}H NMR (250 MHz, $CDCl_3$, TMS): δ_H 2.48 (*s*, 3H, C**H**$_3$), 3.79 (*s*, 6H, 2OC**H**$_3$), 6.45 (*d*, *J* = 2.1 Hz, 2H, 2Ar**H**), 6.58 (*t*, *J* = 2.1 Hz, 1H, 1Ar**H**), 7.37−7.40 (*AA′XX′ system*, 2H, 2Ar**H**), 7.86−7.90 (*AA′XX′ system*, 2H, 2Ar**H**) ppm. ^{13}C NMR (62.5 MHz, $CDCl_3$): δ_C 22.2 (**C**H$_3$), 55.9 (2O**C**H$_3$), 103.7 (Ar**C**H), 106.7 (2Ar**C**H), 119.9 (*q*, *J* = 277.5 Hz, **C**F$_3$), 126.4 (Ar**C**C), 129.7 (2Ar**C**H), 130.3 (2Ar**C**H), 131.6 (Ar**C**C), 146.6 (Ar**C**S), 154.5 (*q*, *J* = 33.7 Hz, **C**O), 161.3 (2Ar**C**O) ppm. ^{19}F NMR (235 MHz, $CDCl_3$): δ_F −67.5 (*s*, C**F**$_3$) ppm. IR υ_{max}/cm^{-1} (thin film): 1160, 1181, 1196, 1292, 1388, 1457, 1595. CI-MS ([M]$^+$) calculated for $C_{17}H_{16}F_3NO_5S$: 403.0701; found: 403.0709.

Synthesis of 3-(3,5-Dimethoxyphenyl)-3-(trifluoromethyl)-diaziridine 20. *O*-Tosyl-2,2,2-trifluoro-1-(3,5-dimethoxyphenyl)-ethanone oxime **17** (15.4 g, 38.2 mmol) was dissolved in dichloromethane (80 mL) and added dropwise over a period of 30 min to liquid ammonia (200 mL) at −78 °C under argon. After 12 h the mixture was warmed to room temperature. Water (200 mL) and dichloromethane (100 mL) were added, and the mixture was stirred for 1 h. The organic phase was removed, and the aqueous phase was extracted with dichloromethane (4 × 150 mL). The combined organic extracts were dried ($MgSO_4$), filtered, and concentrated in vacuo to afford 3-(3,5-dimethoxyphenyl)-3-(trifluoromethyl)diaziridine **20** as a colorless solid, 9.40 g (99%); mp 97−98 °C. ^{1}H NMR (250 MHz, $CDCl_3$, TMS): δ_H 2.24 (*d*, *J* = 8.5 Hz, 1H, N**H**), 2.76 (*d*, *J* = 8.5 Hz, 1H, N**H**), 3.80 (*s*, 6H, 2OC**H**$_3$), 6.51 (*t*, *J* = 2.3 Hz, 1H, Ar**H**), 6.76 (*d*, *J* = 2.3 Hz, 2H, 2Ar**H**) ppm. ^{13}C NMR (62.5 MHz, $CDCl_3$): δ_C 55.9 (2O**C**H$_3$), 58.5 (*q*, *J* = 36.0 Hz, **C**N$_2$), 102.5 (Ar**C**H), 106.5 (2Ar**C**H), 123.8 (*q*, *J* = 278.3 Hz, **C**F$_3$), 134.0 (Ar**C**C), 161.3 (2Ar**C**O) ppm. ^{19}F NMR (235 MHz, $CDCl_3$): δ_F −75.9 (*s*, C**F**$_3$) ppm. IR υ_{max}/cm^{-1} (thin film): 1065, 1158, 1208, 1429, 1462, 1600, 3257. CI-MS ([M]$^+$) calculated for $C_{10}H_{11}F_3N_2O_2$: 248.0773; found: 248.0771.

Synthesis of 3-(3,5-Dimethoxyphenyl)-3-(trifluoromethyl)-diazirine 23. 3-(Trifluoromethyl)-3-(3,5-dimethoxyphenyl)diaziridine **20** (9.40 g, 37.9 mmol) was dissolved in diethyl ether (150 mL), and Ag_2O (11.6 g, 49.8 mmol) was added. The mixture was then stirred vigorously in the dark under argon for 48 h. The insoluble silver residues were removed by filtration though a $MgSO_4$/Celite layered sinter bed and the filtrate was concentrated in vacuo to afford 3-(3,5-dimethoxyphenyl)-3-(trifluoromethyl)-diazirine **23** as a very pale yellow oil, 9.28 g (99%). ^{1}H NMR (250 MHz, $CDCl_3$, TMS): δ_H 3.78 (*s*, 6H, 2OC**H**$_3$), 6.28−6.29 (*m*, 2H, 2Ar**H**), 6.48 (*t*, *J* = 2.2 Hz, 1H, Ar**H**) ppm. ^{13}C NMR (62.5 MHz, $CDCl_3$): δ_C 28.9 (*q*, *J* = 40.3 Hz, 2**C**N$_2$), 55.8 (2O**C**H$_3$), 101.9 (Ar**C**H), 105.1 (2Ar**C**H), 122.4 (*q*, *J* = 274.7 Hz, **C**F$_3$), 131.5 (Ar**C**C), 161.5 (2Ar**C**O) ppm. ^{19}F NMR (235 MHz, $CDCl_3$): δ_F −65.5 (*s*, C**F**$_3$) ppm. IR υ_{max}/cm^{-1} (thin film): 1000, 1159, 1209, 1294, 1460, 1598, 1610, 2943. UV−vis (MeOH): λ = 353.9 (N═N) nm. CI-MS ([M]$^+$) calculated for $C_{10}H_9F_3N_2O_2$: 246.0616; found: 246.0609.

General Procedure for the Synthesis of Polyethers. *Photochemical Polymerization*. The diazirine was weighed into a dry screw-top vial (3 mL), and for solution-phase polymerizations the required amount of anhydrous solvent and a stirrer bar were added. The vials were flushed with argon, sealed, and then placed 2 cm away from a 125 W high-pressure mercury lamp equipped with a water cooling jacket and irradiated for 24 h. After photolysis the solvent was removed from solution-phase polymerization mixtures, and the residue was dried in vacuo (0.1 mbar) at 50 °C for 12 h to yield the desired polymers. The polymers were analyzed using IR, UV−vis, and NMR spectroscopic analyses, and the molecular weight characteristics were determined using GPC coupled with RI detection.

Thermal Treatment. The polymer was weighted into a dry vial (3 mL) that was placed in a drying tube surrounded by a heating jacket. The vials were then heated at 140 °C in vacuo (0.1 mbar) for 12 h to afford glassy solids. The resulting polymeric materials

were analyzed using IR, UV−vis, and NMR spectroscopic analyses, and the molecular weight characteristics were determined using GPC coupled with RI detection.

Characterization of Poly(aryl ether) P1.2a. The analytical data presented are for the poly(aryl ether) **P1.2a** and are representative of the all the poly(aryl ether)s synthesized from the AB-type phenolic monomer **1**. The poly(aryl ether) **P1.2a** was obtained as a yellow/brown solid in a yield of 96%. ^{1}H NMR (250 MHz, d_6-DMSO): δ_H 1.23−1.59 (*m*), 4.06−4.69 (*m*), 5.05−5.57 (*m*), 5.66−5.79 (*m*), 6.31−6.39 (*m*), 6.39−7.49 (*m*), 9.13−9.59 (*m*) ppm. ^{13}C NMR (62.8 MHz, d_6-DMSO): δ_C 25.0−25.5 (*m*), 31.4 (*s*), 38.8 (*s*), 77.0−77.7 (*m*), 113.8−120.8 (*m*), 129.9−131.2 (*m*), 138.6−138.7 (*m*), 145.0 (*s*), 145.7 (*s*), 146.3−147.5 (*m*), 159.0−159.3 (*m*), 159.8−160.2 (*m*) ppm. IR υ_{max}/cm^{-1} (thin film): 1019, 1071, 1159, 1252, 1371, 1449, 1487, 1597, 2870, 2976, 3335. UV−vis (MeOH): λ = 201, 275 nm. GPC (0.05 M LiBr in DMF, 60 °C): M_w = 1.6 kDa, M_n = 0.7 kDa, PDI = 2.3.

Characterization of Poly(aryl ether) P2.3a. The analytical data presented are for the poly(aryl ether) **P2.3a** and are representative of the all the poly(aryl ether)s synthesized from the AB-type phenolic monomer **2**. The poly(aryl ether) **P2.3a** was obtained as a yellow/brown solid in a yield of 98%. ^{1}H NMR (250 MHz, d_6-DMSO): δ_H 4.92−5.62 (*m*), 5.92−6.42 (*m*), 6.49−7.89 (*m*), 9.30−10.4 (*m*) ppm; ^{13}C NMR (62.8 MHz, d_6-DMSO) δ_C 30.8 (*s*), 34.8 (*s*), 71.0 (*s*), 114.8−115.3 (*m*), 115.9−116.4 (*m*), 116.9−117.4 (*m*), 118.2−119.1 (*m*), 128.7−130.6 (*m*), 137.6 (*s*), 157.4−158.0 (*m*) ppm. ^{19}F NMR (235 MHz, d_6-DMSO): δ_F −62.9 to −62.5 (*m*), −65.9 to −64.0 (*m*), −67.1 to −66.6 (*m*), −67.9 to −67.4 (*m*), −68.2 to −68.1 (*m*), −70.9 (*s*), −71.0 (*s*), −71.1 (*s*), −74.9 (*s*), −75.4 (*d*), −76.4 to −75.5 (*m*), −77.4 to −77.0 (*m*), −78.1 to −78.0 (*m*), −83.3 to −83.1 (*m*) ppm. IR υ_{max}/cm^{-1} (thin film): 1070, 1141, 1165, 1252, 1455, 1593, 2980, 3320. UV−vis (MeOH): λ = 201, 278 nm. GPC (0.05 M LiBr in DMF, 60 °C): M_w = 11.0 kDa, M_n = 3.7 kDa, PDI = 3.0.

Characterization of Poly(aryl ether) P3.3a. The analytical data presented are for the poly(aryl ether) **P3.3a** and are representative of the all the poly(aryl ether)s synthesized from the AB_2-type phenolic monomer **3**. The poly(aryl ether) **P3.3a** was obtained as a yellow/brown solid in a yield of 99%. ^{1}H NMR (250 MHz, d_6-DMSO): δ_H 4.15 (*br s*), 4.57 (*q*), 4.91 (*q*), 5.05−5.63 (*br s*), 5.68−7.03 (*m*), 7.25−7.51 (*m*), 7.58−7.76 (*m*), 8.85−10.2 (*m*), 10.2 (*br s*) ppm. ^{13}C NMR (62.8 MHz, d_6-DMSO): δ_C 30.8 (*s*), 34.2 (*s*), 34.8 (*s*), 71.0 (*s*), 103.1 (*s*), 102.3 (*s*), 106.1−106.3 (*m*), 138.1 (*s*), 140.8 (*s*), 158.1 (*s*), 158.5 (*s*), 158.9−159.1 (*m*). ^{19}F NMR (235 MHz, d_6-DMSO): δ_F −61.6 to −61.2 (*m*), −62.7 to −62.6 (*m*), −65.0 to −64.2 (*m*), −67.1 to −66.4 (*m*), −67.9 to −67.8 (*m*), −70.8 (*s*), −74.7 to −74.5 (*m*), −76.1 to −75.2 (*m*), −77.1 to −76.9 (*m*), −77.9 to −78.2 (*m*), −83.3 to −83.1 (*m*) ppm. IR υ_{max}/cm^{-1} (thin film): 1011, 1159, 1266, 1347, 1462, 1607, 2981, 3345. UV−vis (MeOH): λ = 202, 282 nm. GPC (0.05 M LiBr in DMF, 60 °C): M_w = 6.1 kDa, M_n = 3.0 kDa, PDI = 2.0.

Characterization of Poly(benzyl ether) P4.2a. The analytical data presented are for the poly(benzyl ether) **P4.2a** and are representative of the all the poly(benzyl ether)s synthesized from the AB-type benzyl alcohol monomer **4**. The poly(benzyl ether) **P4.2a** was obtained as a cream solid in a yield of 97%. ^{1}H NMR (250 MHz, d_6-DMSO): δ_H 0.99−1.00 (*m*), 1.62 (*br s*), 1.65 (*br s*), 2.08 (*s*), 2.31−2.38 (*m*), 2.78 (*br s*), 3.46 (*br s*), 3.53−3.70 (*m*), 3.78 (*br s*), 3.83 (*br s*), 4.25−4.71 (*m*), 5.03−5.45 (*m*), 5.76 (*s*), 6.77−8.17 (*m*), 9.86−9.90 (*m*), 10.0−10.1 (*m*) ppm. ^{13}C NMR (62.8 MHz, d_6-DMSO): δ_C 30.8 (*s*), 62.7 (*s*), 62.9 (*s*), 63.1 (*s*), 71.0−71.9 (*m*), 77.3−79.3 (*m*), 122.0−122.4 (*m*), 126.4−129.3 (*m*), 130.0−130.2 (*m*), 132.4−133.2 (*m*), 137.9−138.3 (*m*), 143.5 (*s*). ^{19}F NMR (235 MHz, d_6-DMSO): δ_F −57.5 to −57.9 (*m*), −62.1 to −62.6 (*m*), −63.0 (*d*), −63.3 (*d*), −63.9 (*s*), −64.1 to −64.4 (*broad s*), −64.8 to −65.0 (*m*), −65.1 to −65.4 (*m*), −66.4 (*d*), −66.5 to −67.3 (*m*), −67.9 (*s*), −67.9 to −68.9 (*m*), −69.6 (*d*), −70.8 to −71.6 (*m*), −71.6 to −72.2 (*m*), −73.0 to −73.4 (*m*), −73.4 to −73.7 (*m*), −74.2 to −74.4 (*m*), −77.0 to −77.5 (*m*), −77.8 to −78.6 (*m*), −78.7 to −78.8 (*m*), −82.0 (*broad s*), −83.1 to −83.4 (*m*) ppm. IR υ_{max}/cm^{-1} (thin film): 1023, 1137, 1163, 1266, 1354, 1450, 1612, 2878, 3402. UV−vis (MeOH): λ = 209, 246 nm. GPC (0.05 M LiBr in DMF, 60 °C): M_w = 14.3 kDa, M_n = 3.7 kDa, PDI = 3.9.

Acknowledgment. This work was supported by a grant to W.H. from the DuPont Young Professor Programme (postgraduate studentship for A.B.). The authors also thank EPSRC (GR/R06441) and Polymer Laboratories Ltd. for the funding provided for the gel permeation facilities at the University of Reading.

Supporting Information Available: Detailed experimental procedures and characterization of compounds **2, 5, 7**, **10**, **12**, **13**, **15**, **16**, **18 19**, **21**, **22**, **24**, and *N*,*N*-diethyltrifluoroacetamide; Figures S1−S10 (high-resolution mass spectra of diazirine monomers **1**−**4** and compounds **6**, **11**, **14**, **17 20**, and **23**), Figures S11−S20 (^{1}H NMR spectra of diazirine monomers **1**−**4** and compounds **6**, **11**, **14**, **17**, **20**, and **23**), Figures S21−S28 (^{19}F NMR spectra of diazirine monomers **2**−**4** and compounds **11**, **14**, **17 20**, and **23**), Figures S29−S39 (GPC chromatograms of polyethers **P1.1a**−**P1.3a**, **P2.1a**−**P2.3a**, **P3.1a**−**P3.3a**, **P4.1a**−**P4.3a**, **P1.1b**−**P1.3b**, **P2.1b**−**P2.3b**, **P3.1b**−**P3.3b**, **P1.4b**−**P1.4e**, **P3.4a**−**P3.4e**, **P4.4a**−**P4.4e**, and **P4.5a**−**P4.5l**), Figures S40−S43 (IR spectra of monomers **1**−**4** and polyethers **P1.3a**, **P1.3b**, **P2.2a**, **P2.2b**, **P3.2a**, **P3.2b**, and **P4.2a**), Figures S44−S46 (UV−vis spectra of monomers **1**−**4** and polyethers **P1.3a**, **P1.3b**, **P2.2a**, **P3.2a**, and **P4.2a**), Figures S47 and S48 (^{1}H NMR spectroscopic data for polyethers **P1.1a**, **P1.1b**, **P1.3a**, and **P1.3b**), Figures S49−S56 (^{19}F NMR spectroscopic data for polyethers **P2.1a**, **P2.1b**, **P2.3a**, **P2.3b**, **P3.1a**, **P3.1b**, **P3.2a**, **P3.2b**, **P3.3a**, **P3.3b**, **P4.1a**, **P4.2a**, and **P4.3a**), Figures S57 (DSC data for polyethers **P1.3a**, **P1.3b**, **P2.2a**, **P2.2b**, **P3.2a**, **P3.2b**, and **P4.2a**), Figure S58 (crystal structure and packing of phenolic diazirine **3**), Tables S1−S6 (crystal data and parameters for phenolic diazirine **3**), and Table S7 (database of ^{19}F NMR chemical shifts for trifluoromethyl groups). This material is available free of charge via the Internet at http://pubs.acs.org.

References and Notes

(1) Doyle, M. P. *React. Intermed. Chem.* **2004**, 561.
(2) Blencowe, A.; Hayes, W. *Soft Matter* **2005**, *1*, 178.
(3) (a) Moloney, M. G.; Ebenezer, W.; Awenat, K. M. Patent: US 6699527, 2000. (b) Awenat, K. M.; Davis, P. J.; Moloney, M. G.; Ebenezer, W. *Chem. Commun.* **2005**, 990.
(4) Blencowe, A.; Cosstick, K.; Hayes, W. *New J. Chem.* **2006**, *1*, 53.
(5) Meerwein, H. *Angew. Chem.* **1948**, *60*, 78.
(6) Gutsche, C. D.; Kinoshita, K. *J. Org. Chem.* **1963**, *28*, 1762.
(7) Kubota, H.; Morawetz, H. *J. Polym. Sci., Polym. Chem. Ed.* **1967**, *5*, 585.
(8) Kantor, S. W.; Osthoff, R. C. *J. Am. Chem. Soc.* **1953**, *75*, 931.
(9) Imoto, M.; Nakaya, T. *J. Macromol. Sci., Rev. Macromol. Chem.* **1972**, *C7*, 1.
(10) Mucha, M.; Wunderlich, B. *J. Polym. Sci., Polym. Phys.* **1974**, *12*, 1993.
(11) Bawn, C. E. H.; Rhodes, T. B. *Trans. Faraday Soc.* **1954**, *50*, 934.
(12) Van Gaver, G. S.; Magni, R. Patent: FR 1313247, 1962.
(13) Leffler, J. E.; Ramsey, B. G. *Proc. Chem. Soc.* **1961**, 117.
(14) (a) Dorion, G. H.; Polchlopek, S. E.; Sheers, E. H. *Angew. Chem.* **1964**, *76*, 495. (b) Dorion, G. H.; Sheers, E. H. Patent: US 3255124, 1966.
(15) Bawn, C. E. H.; Ledwith, A.; Matthies, P. *J. Polym. Sci.* **1958**, *33*, 21.
(16) Richardson, M. J.; Flory, P. J.; Jackson, J. B. *Polymer* **1963**, *4*, 221.
(17) Buckley, G. D.; Ray, N. H. *J. Chem. Soc.* **1952**, 3701.
(18) Krakovyak, M. G.; Anufrieva, E. V.; Skorokhodov, S. S. Patent: SU 319610, 1971.
(19) Bai, J.; Shea, K. J. *Polym. Prepr.* **2005**, *46*, 765.
(20) Shea, K. J.; Walker, J. W.; Zhu, H.; Paz, M.; Greaves, J. *J. Am. Chem. Soc.* **1997**, *119*, 9049.
(21) Goubeau, P.; Rohwedder, H. *Annalen* **1957**, *604*, 168.
(22) Davies, A. G.; Hare, D. G.; Khan, O. R.; Sikora, J. *J. Chem. Soc.* **1963**, 4461.
(23) Bawn, C. E. H.; Ledwith, A.; Matthies, P. *J. Polym. Sci.* **1958**, *34*, 93.
(24) Werner, H.; Richards, J. H. *J. Am. Chem. Soc.* **1968**, *90*, 4976.

(25) Feltzin, J.; Restaino, A. J.; Mesrobian, R. B. *J. Am. Chem. Soc*. **1955**, *77*, 206.
(26) (a) Nasini, A. G.; Trossarelli, L.; Saini, G. *Makromol. Chem.* **1961**, *550*, 44−46. (b) Nasini, A. G.; Saini, G.; Trossarelli, L. *Pure Appl. Chem.* **1962**, *4*, 255.
(27) McCrindle, R.; Arsenault, G. J.; Farwaha, R.; Hampden-Smith, M. J.; McAlees, A. J. *J. Chem. Soc., Chem. Commun.* **1986**, 943.
(28) Fischer, F.; Tropsch, H. *Brennst.-Chem.* **1926**, *7*, 96.
(29) Brady, R. C.; Pettit, R. *J. Am. Chem. Soc.* **1980**, *102*, 6182.
(30) (a) Hermans, J. C.; Smets, G. J. Patent: GB 1142165, 1969. (b) Smets, G. J.; Bracke, W.; Hermans, J. C. *Pure Appl. Chem.* **1969**, *15*, 525.
(31) Richards, F. M.; Lamed, R.; Wynn, R.; Patel, D.; Olack, G. *Protein Sci.* **2000**, *9*, 2506.
(32) Bruce, J. M.; Creed, D.; Dawes, K. *J. Chem. Soc. (C)* **1971**, 2244.
(33) Beumer, R.; Bayon, P.; Bugada, P.; Ducki, S.; Mongelli, N.; Sirtori, F. R.; Telser, J.; Gennari, C. *Tetrahedron* **2003**, *59*, 8803.
(34) (a) Brunner, J.; Senn, H.; Richards, F. M. *J. Biol. Chem.* **1980**, *255*, 3313. (b) Bennett, P.; Harwood, L. M.; Macro, J.; McGregor, A. *J. Chem. Soc., Chem. Commun.* **1994**, 961.
(35) (a) Jennings, B. M.; Liu, M. T. H. *J. Am. Chem. Soc*. **1976**, *98*, 6416. (b) Liu, M. T. H.; Ramakrishnan, K. *J. Org. Chem.* **1977**, *42*, 3450.
(36) (a) Doyle, M. P.; Devia, A. H.; Bassett, K. E.; Terpstra, J. W.; Mahapatro, S. N. *J. Org. Chem.* **1987**, *52*, 1619. (b) Bonneau, R.; Liu, M. T. H. *J. Phys. Chem. A* **2000**, *104*, 4115.
(37) *Reactive Intermediate Chemistry*; Moss, R., Platz, M. S., Jones, M., Eds.; Wiley: Hoboken, NJ, 2004.
(38) (a) Richard, J. P. *J. Am. Chem. Soc.* **1989**, *111*, 1455. (b) Richard, J. P. *J. Am. Chem. Soc*. **1989**, *111*, 6735. (c) Richard, J. P.; Amges, T. L.; Vontor, T. *J. Am. Chem. Soc.* **1992**, *114*, 5626.
(39) Tusji, Y.; Toteva, M. M.; Garth, H. A.; Richard, J. P. *J. Am. Chem. Soc.* **2003**, *125*, 15455.
(40) Brahms, D. L. S.; Dailey, W. P. *Chem. Rev.* **1996**, *96*, 1585.
(41) A database of ^{19}F NMR shift values and coupling constants for trifluoromethyl groups is provided in the Supporting Information.
(42) (a) Hawker, C. J.; Fréchet, J. M. J.; Grubbs, R. B.; Dao, J. *J. Am. Chem. Soc.* **1995**, *117*, 10763. (b) Fréchet, J. M. J.; Henmi, M.; Gitsov, I.; Aoshima, S.; Leduc, M. R.; Grubbs, R. B. *Science* **1995**, *269*, 1080.
(43) Crystallographic data for compound **3** are provided in the Supporting Information.

MA061951L